EFDA–JET–PR(10)27

J.Garcia, G. Giruzzi, X. Litaudon, J. Mailloux, M. Goniche, J.F. Artaud,
V. Basiuk, J. Decker, F. Imbeaux, Y. Peysson, M. Schneider
and the JET EFDA contributors

# Impact of Off-Axis RF Current Drive on JET Advanced Scenarios

"This document is intended for publication in the open literature. It is made available on the understanding that it may not be further circulated and extracts or references may not be published prior to publication of the original when applicable, or without the consent of the Publications Officer, EFDA, Culham Science Centre, Abingdon, Oxon, OX14 3DB, UK."

"Enquiries about Copyright and reproduction should be addressed to the Publications Officer, EFDA, Culham Science Centre, Abingdon, Oxon, OX14 3DB, UK."

The contents of this preprint and all other JET EFDA Preprints and Conference Papers are available to view online free at www.iop.org/Jet. This site has full search facilities and e-mail alert options. The diagrams contained within the PDFs on this site are hyperlinked from the year 1996 onwards.

# Impact of Off-Axis RF Current Drive on JET Advanced Scenarios

J.Garcia, G. Giruzzi, X. Litaudon, J. Mailloux[1], M. Goniche, J.F. Artaud,
V. Basiuk, J. Decker, F. Imbeaux, Y. Peysson, M. Schneider
and the JET EFDA contributors*

***JET-EFDA, Culham Science Centre, OX14 3DB, Abingdon, UK***

*[1]CEA, IRFM, F-13108 Saint-Paul-lez-Durance, France*
*[2]EURATOM-CCFE Fusion Association, Culham Science Centre, OX14 3DB, Abingdon, OXON, UK*
** See annex of F. Romanelli et al, "Overview of JET Results",*
*(Proc. 22 nd IAEA Fusion Energy Conference, Geneva, Switzerland (2008)).*

Preprint of Paper to be submitted for publication in
Nuclear Fusion

**ABSTRACT.**
The impact of the Radio Frequency heating and current drive systems on JET advanced scenarios at high density is analyzed by means of the CRONOS suite of codes for integrated tokamak modelling. In particular, the performance of the proposed Electron Cyclotron heating and current drive system for JET is evaluated. As a first step, the code is applied in the interpretative mode to analyze two high power advanced scenario discharges of JET, in order to validate both the heating and current drive computational modules and the overall simulation procedure. Then, JET advanced scenarios are studied by predictive simulations on the basis of previous results. The simulations show that Lower Hybrid and Electron Cyclotron heating and current drive systems can provide together off-axis current in order to create and sustain steady-state scenarios on JET at high density. These results give deeper insight into the future advanced scenarios in ITER.

## 1. INTRODUCTION

An important goal of the magnetically confined nuclear fusion research program is to develop advanced scenarios with zero loop voltage and significant fusion power production that could project to a steady-state reactor. These advanced scenarios rely on the capability for controlling both the pressure and the current density profile. Moreover, the power source that sustains the burn must be partly generated by the plasma itself, via self-heating due to the energetic alpha particles produced by the fusion reactions. In addition, a large fraction of the current flowing in the plasma and necessary for the stability of the magnetic configuration should also be self-generated by the bootstrap effect (at least 50% [1]). This implies that a localised control of heating, current drive and bootstrap current is necessary to sustain these scenarios for a long time. However, this is notoriously difficult when the bootstrap fraction is the dominant contribution (current alignment problem). These inherent difficulties will fully arise in the D-T phase in ITER, since, for the first time, a significant amount of alpha power will be obtained for long times, which will require of precise current and pressure control in advanced scenario regimes.

Present day tokamak experiments close to ITER conditions can effectively give a deeper insight into the problem of current and heating channels control in advanced conditions, improving the present knowledge of all these effects. For this purpose, the 2009 JET campaign has been focused on the analysis of advanced tokamak scenarios (hybrid and steady-state) with ITER relevant characteristics, in particular with a high electron density which will be more suitable for future JET campaigns working with the ITER Like Wall (ILW). However, one of the main characteristics of ITER steady-state scenarios, i.e. the necessity of off-axis current to create and sustain them [2,3,4], is difficult to obtain in JET due to the lack of enough off-axis current sources. In addition, this problem is amplified in the high density regimes, where the current drive efficiency is lower. The inclusion of an Electron Cyclotron Resonant Heating and Current Drive (ECRH/ECCD) system could increase the JET performance in two different ways, one is by increasing the electron temperature in the core in order to work with similar electron and ion temperatures and second by increasing

the off-axis current drive capability. This last feature could be essential for the establishment of ITER relevant steady-state scenarios.

The analysis of experimental shots with transport codes is also an important point in order to check different plasma characteristics as: heating coupling to electrons and ions, non-inductive current and bootstrap current fractions, radiated power, internal inductance, loop voltage, etc. With this information, future experimental campaigns can be better conceived in order to accomplish the goal of having realistic steady-state scenarios, approaching, as well as possible, ITER-like conditions.

In this paper the integrated tokamak modelling suite of codes CRONOS [5] is applied to analyze two different advanced discharges at high power and high plasma performance, Pulse No: 77895 and Pulse No: 78052, from the 2009 campaign of JET. These shots are considered here as representatives of the advanced JET scenarios at high density, since high input power was used (≈30MW) and high $\beta_N$ and bootstrap current fraction were obtained. Therefore, they seem suitable to analyze the impact of off-axis current on advanced scenarios on JET. At first, an interpretative analysis has been carried out in order to be used for validation of the various modules entering the CRONOS suite, in particular with respect of their goodness for JET experimental conditions. This gives an overview of the current distribution in the discharges, underlining the difficulty to maintain a steady current profile on resistive time scales. A fully predictive simulation has then been done with the Bohm-GyroBohm transport model [6], in order to allow sensitivity analyses of these shots. Finally, the impact of adding an extra source of off-axis CD, e.g., ECRH/ECCD to improve the performances of such advanced scenarios on JET has been investigated.

## 2. MODELLING ASSUMPTIONS

These studies have been performed by means of the CRONOS suite of codes, which can solve the transport equations for various plasma fluid quantities (current, energy, particles, momentum). This is done in one dimension (the toroidal magnetic flux coordinate), self-consistently with 2-dimensional magnetic equilibrium which is calculated by means of the HELENA code [7]. The neoclassical terms, and in particular the bootstrap current which is essential for the correct simulation of the steady-state regimes, are determined using the NCLASS [8] code. The sources are computed by external modules coupled with the main transport equations. The Neutral Beam Current Drive (NBCD) is computed by means of the NEMO/SPOT code [9], including calculations of the fast ions distribution by the orbit-following Monte Carlo code SPOT [10]. The ECRH/ECCD is calculated by means of REMA [8] (ray-tracing and relativistic damping of electron cyclotron waves), with a linear estimate of the ECCD efficiency [12]. The Lower Hybrid (LH) power deposition and driven current have been computed inside CRONOS by means of the LUKE/C3PO code [13], i.e., a 3D Fokker-Planck code coupled to toroidal ray-tracing. The Ion Cyclotron Heating source is computed by the PION code [14], a time dependent 1-D Fokker Planck, including collisions and fast ion orbit losses. The core plasma line and bremsstrahlung radiation are computed with a model based on coronal equilibrium [15].

## 3. INTERPRETATIVE ANALYSIS OF THE JET ADVANCED PULSE NO'S: 78052 AND 77895

A specific evaluation of the CRONOS capability to simulate JET advanced scenarios experiments has been performed. In particular, the Pulse No's: 77895 and 78052 have been analyzed by means of interpretative simulations, i.e., coupled current diffusion and equilibrium calculations with fixed density and temperature profiles, obtained by fits of the experimental measurements.

The main characteristics of Pulse No's 77895 and 78052 are shown in table 1 and the time evolution of the main plasma parameters are shown in figure 1.

### *3.1 ANALYSIS OF PULSE NO: 77895*

For this discharge, 23MW of NBI, 6MW of ICRH and 2MW of LH were used. In the case of the LH, we use a simple n|| spectrum with a gaussian shape centered on $n_{||} = 2.1$, which is the n|| used in the experiment. First, an interpretative simulation of the shot has been done by using the experimental data available (density and temperature profiles, plasma boundary) and simulating the evolution of the current density profiles. In figure 2, the experimental temperatures and electron density (obtained with High Resolution Thomson Scattering (HRTS) and Charge-Exchange spectroscopy (CXFM)) as well as the calculated current density profiles obtained with CRONOS are shown at t = 6s. The current density profile is mainly determined by the bootstrap current and NBCD in the plasma center, the LH at $\rho = 0.65$ and by the bootstrap current in the pedestal region. In figure 3, the time evolution of the total currents as well as the total non-inductive, including bootstrap current, ($f_{ni}$) and bootstrap current fractions ($f_{bs}$) are shown. There is a clear evolution of the total non-inductive current ($I_{ni}$) and bootstrap current ($I_{bs}$). At the beginning of the flat-top phase $I_{ni} = 1.2$MA and $I_{boot} = 0.75$ MA which represents $f_{ni} = 69\%$ and $f_{boot} = 43\%$, whereas at the end, $I_{ni} = 1.1$MA, $I_{boot} = 0.6$ MA with $f_{ni} = 63\%$ and $f_{boot} = 37\%$. The total LH current obtained varies in the range $I_{lh} = 0.15$-$0.18$ MA and the NBCD is $I_{nbi} = 0.25$MA. In order to verify these values with experimental data, in figure 4 the loop voltage, $V_{loop}$, and the internal inductance (li3) calculated with CRONOS are compared with those obtained with EFIT. In the case of li, the agreement is quite good whereas in the case of $V_{loop}$ the general trend is well reproduced (slight increase in the flat top phase). Regarding the time evolution of the q profile, both current diffusion calculations with CRONOS and equilibrium reconstructions obtained with EFIT constrained by MSE angles and total pressure are shown in figure 5. Just after the L-H transition, the q profile is already slightly below 2 according to the MSE data. After that, it keeps dropping slowly and after the power flattop phase it is close to 1. Therefore, according to these calculations, this scenario is not well sustained due to the current penetration and the lack of enough bootstrap and off-axis currents. The results obtained with CRONOS and the MSE constrained EFIT agree in this general trend.

### *3.2 ANALYSIS OF PULSE NO: 78052*

This shot has similar characteristics to 77895. However, at t=8.2s, half of the NBI power is lost

(octant 8 drops out) which degrades the global performance. Therefore, the interpretative analysis is carried out here until t = 8s. The main characteristics of Pulse No: 78052 can be found in table 1. For this shot 23MW of NBI, 5MW of ICRH and 2MW of LH (with $n_{||} = 1.8$) were used. In figure 6, the experimental temperatures and electron density as well as the calculated current density profiles obtained with CRONOS are shown at t = 6.0s. The current density profile is determined by the bootstrap current and NBCD in the plasma center and by the bootstrap current at the edge. An important difference with respect to Pulse No: 77895 is that in this case no LH penetration is found, since $n_{||}$ was too low for accessibility at the density considered. One way to overcome this issue could to be to increase $n_{||}$ up to 2.1 (like in the previous shot) or to decrease the electron density. This has some impact on the total non-inductive current obtained, since, as shown in figure 7, $I_{ni} = 0.9$MA with $f_{ni} = 69\%$, which is lower than for the previous shot. The bootstrap current is also slightly lower, $I_{bs} = 0.68$MA with $f_{boot} = 40\%$ due to the lower ion temperature obtained. However, in this case both quantities remain more stable than in the previous case and no significant decrease of $f_{ni}$ or $f_{boot}$ is observed before the onset of the MHD mode. Finally, $I_{nbi} = 0.24$MA, as in the previous shot. The evolution of the q profile follows the same trend as the one obtained previously. From an initial q profile close to 2, it drops during the discharge and the final state is close to 1.

Finally, the comparison between li and $V_{loop}$ calculated with EFIT and CRONOS is shown in figure 8, revealing a good agreement between experiment and simulation.

### *3.3 SUMMARY OF INTERPRETATIVE ANALYSIS OF PULSE NO'S: 78052 AND 77895*

From the previously shown analysis, some common characteristics can be inferred for Pulse No's: 78052 and 77895. At the beginning of the flat-top phase the q profile is close to 2, however, it cannot be sustained for the full discharge and at the end the q profile remains close to 1 (and could be even lower since the scenarios are not yet in steady-state due to the limitation of the duration of the shots compared to the resistive time, ≈7s). This feature is related to the fact that the non-inductive current level is not sufficient, since, although on average $f_{boot} = 40\%$ and $f_{ni} = 70\%$ for both shots, the bootstrap current fraction is too low, the NBCD is rather peaked on-axis (which contributes to the dropping of the core q profile) and the LH contribution is very little (less than 10%). Therefore, in order to get a steady-state scenario with q>2 and $f_{ni} = 100\%$ (as the one expected for ITER), either more bootstrap current must be obtained or more auxiliary noninductive current must be driven, which in turn should be off-axis in order to balance the large on-axis current already generated by NBCD. This possibility will be analyzed in section 5, however, since this implies full predictive simulations, a predictive simulation will be carried out first for Pulse No: 77895 in section 4 in order to check the validity of the different assumptions employed.

Finally, the results obtained with the CRONOS code have shown that the evolution of li, $V_{loop}$ and the q profile is in agreement with those obtained with EFIT, showing that the code is ready to simulate advanced scenarios on JET.

## 4. PREDICTIVE ANALYSIS OF PULSE NO: 77895

With the aim of analyzing the temperatures that could be obtained by changing some of the main characteristics of the Pulse No: 77895, a predictive simulation of the temperatures and currents evolution has been carried out with the Bohm-GyroBohm model which was formerly established from the analysis of a large number of JET discharges. Since an ITB is observed in the ion channel, the criterion for the ITB triggering based on a combination of magnetic and E × B shear is also used in the following way. The ITBs are introduced with the function $1/(1+\exp(20(0.05 + \omega_{E\times B}/ \gamma_{ITG} - s)))$ multiplying the Bohm transport coefficient. Here, $\omega_{E\times B}$ is the flow shearing rate by Hahm–Burrell [16], s the magnetic shear and $\gamma_{ITG}$ is a simple approximation of the linear growth rate defined as $\gamma_{ITG} = v_{th,i} /R$ with $v_{th,i}$ being the ion thermal velocity and R the major radius. The $\omega_{E\times B}$ shearing rate is calculated by using the experimental rotation. Essentially, this function is a Heaviside function with argument $C_1 + s - C_3\ \omega_{E\times B}/ \gamma_{ITG}$, which has been already used to simulated ITB plasmas on JET [17] with the Bohm-GyroBohm transport model. Basically, when the argument $0.05 + \omega_{E\times B}/ \gamma_{ITG} - s$ changes its sign, the ITB either forms $(0.05 + \omega_{E\times B}/\gamma_{ITG} - s > 0)$ or $(0.05 + \omega_{E\times B}/\gamma_{ITG} - s < 0)$ collapses. Physically, when the Bohm-type of anomalous transport is fully suppressed the ITB forms.

The pedestal width has been fixed to the experimental data whereas the height is calculated in such a way that the pedestal energy content, $w_{ped}$, is $w_{ped}=w_{tot}-w_{core}$, where the total energy content, $w_{tot}$, follows the ITERH-98(y,2) scaling whereas the core content, $w_{core}$, follows the ITER97-L scaling [18]. This methodology is described in detail in [19].

In figure 9, the simulated ion and electron temperatures are compared to the experimental data at t = 6s and the time evolution of the central temperatures is also shown. The profiles are in reasonable agreement as well as the central temperature evolution. The analysis of the power density profiles for ions and electrons are shown in figure 10. It is found that the main NBI power is coupled to the ions. On the other hand, the ICRH power is mainly on-axis for the electrons, however this does not compensate for the low NBI power coupled, and that is the reason why in this shot the ion temperature is higher than the electron one for $\rho<0.5$. The total ohmic and bootstrap currents are also well simulated as shown in figure 11. Finally, the comparison between the simulated li and that obtained with EFIT is shown in figure 12. Although the temperature pedestal height is well simulated for electrons and ions, slightly differences in the profile appear in that region which finally lead to some differences in the value of li compared to experimental data, mainly due to the differences on the bootstrap current at the edge (being more important at the LH transition). In any case, the trend is very similar in both cases. Therefore, this model gives reasonable results for the temperature profiles and can be used to analyze the impact of adding an extra source of off-axis CD, in order to control the current alignment and increase the bootstrap fraction.

## 5. ANALYSIS OF THE IMPACT OF OFF-AXIS CURRENT ON SHOT 77895

With the aim of analyzing whether the inclusion of more off-axis current could lead to a steady-state scenario, the inclusion of an ECRH/ECCD system, consistent with the proposed configuration for

JET [20], is considered. Here, the ECRH/ECCD power used is $P_{EC}$ = 10MW (170 Ghz, X-mode, 2nd harmonic), with two launching mirrors (5 MW each) located at major radius R = 4.32m and height Z = –0.4m for mirror 1 and Z=-0.3m for mirror 2. The poloidal injection angle is $\theta$ = –5° for mirror 1 and $\theta$ = –8° for mirror 2 whereas the toroidal angle is $\phi$ = 25° for both. With this configuration, the deposition is located at $\rho \sim 0.6$ as shown in figure 13. In addition, since it is well known that the tailoring of the q profile by localised CD can be optimised by applying the wave power during the initial current ramp-up phase of the discharge, this technique is used here.

In order to explore the impact of this technique on advanced JET discharges, CRONOS predictive simulations have been performed with the same parameters used for Pulse No: 77895, but applying LHCD earlier in the ramp-up phase (t = 2s). With the aim of analyzing the different impact of LHCD and ECRH/ECCD powers two scenarios have been considered: one with only 2MW of LHCD (as in the original shot) but included in the ramp-up phase (Scenario 1) and another one with the same LHCD power scheme but with 5MW of ECRH in the ramp-up and 10 MW of ECRH/ECCD in the flat-top phase (Scenario 2). In the case of scenario 2, the LH current is quickly located at $\rho \sim 0.6$, since the electron temperature is increased at that point due to the addition of the ECRH power as shown in figure 15. Therefore, with the aim of comparing the impact of more off-axis current and for simplicity, the LH deposition has been fixed at $\rho \sim 0.6$ for both scenarios with the current drive efficiency previously calculated for Pulse No: 77895 (and therefore no synergy between LH and ECCD has been taken into account). The density and toroidal velocity profiles are also kept from the experimental Pulse No: 77895.

The temperature profiles obtained in both scenarios at t = 6s as well as the evolution of central electron and ion temperatures are shown in figure 14. It appears that the strong increase of the temperature at t = 4-5s can be kept steadily in time by the effect of ECCD, whereas it decays without EC power. This temperature increase is in fact related to the formation of an ITB on the ion channel. As shown in figure 15, this ITB formation is linked to the appearance of a region with negative magnetic shear together with the rotation induced by the NBI power. However, in scenario 1, the q profile is initially well reversed, owing to the application of LHCD in the ramp-up phase, but it subsequently evolves into a monotonic one, as already observed in JET [21]. Conversely, ECCD is able to keep the q profile reversed and the ITB erosion due to current diffusion is strongly reduced. As a result, the non-inductive current fraction remains very close to one, whereas for scenario 1 it drops to 70%, the same value obtained when LHCD is applied at the end of the ramp-up. The non-inductive current fraction also benefits from the increase of bootstrap fraction (> 50 %), as shown in figure 16. The current density profiles obtained at t=6s for scenario 2 are shown in figure 16. It appears that the bootstrap current increase comes from the foot of the ITB, which, in the flat-top phase, is mainly sustained by the ECCD current, which provides enough negative shear to sustain the scenario, owing to its narrow profile. A similar scenario was obtained by using more NBI power as well as more LHCD to create and sustain an ITB at $\rho \sim 0.7$ [22,23]. This type of effects of interplay between current profile diffusion and ITB strength and sustainment are exactly those involved in the

sustainment of ITBs in the ITER steady-state regimes [24]. In fact, scenario 1 shows that the tailoring of the q profile in the ramp-up phase does not necessarily lead to an improved scenario with ITB , since scenario 1 and the original Pulse No: 77895 are very similar from t>6s. Conversely, in scenario 2, the combined effect of LH+ECCD is able to tailor the q profile in the ramp-up phase and to sustain it above 2 for the time considered here. This approach for steady-state scenario establishment has been already pointed out to be important for ITER in [24-26]. Therefore, its investigation in JET would be of great relevance for the development of ITER steady-state scenarios.

The impact of the ITB on scenario 2 is evaluated in figure 17 by removing the factor responsible for the turbulent transport reduction on the Bohm-gyroBohm transport model. The bootstrap current is reduced by a 25% and therefore the total non-inductive current fraction, which was close to 100%, is reduced to 80%. However, the impact on the evolution of the q profile is not so important as also shown in figure 17. At t = 10s, the q profile in the case with ITB is still above 2 and in the case with no ITB it is just slightly below 2. This fact shows that the real controller of the q profile is the ECRH/ECCD, since in the case of scenario 1, there was no ITB either at t=10s but the q profile was well below 2.

In any case, the analysis performed here has been done for the duration of the original shot 77895 with the aim of making the full comparison during the original configuration. However, in order to know whether these scenarios are really steady-state, longer simulations are needed since the sustainability of ITB plasmas involve several current diffusion times [24]. Therefore, scenario 2 has been extended until 20s with the aim of analyzing this problem. As shown in figure 18, the q profile, which at t=10s is above 2, drops very slowly and at t = 20s is close to 1.5. Therefore, the combination of ECCD+LH significantly slows down the current evolution, however, with the configuration used here, no completely steady-state scenario can be achieved. Anyway, more analysis must be done in order to study whether with another heating configuration (mainly the ECCD location) this behavior can be overcome. Finally, these features show that longer experiments would be needed in order to guarantee that the scenarios analyzed on JET can be sustained for much longer times of the order of several current diffusion times.

## 6. SUMMARY AND CONCLUSIONS

An analysis of the possible development of steady-state scenarios on JET with high densities has been carried out with the CRONOS suite of codes. Similar conclusions have been obtained from the interpretative analysis of Pulse No's: 78052 and 77895. Although almost the full power capability of JET has been used, still the desired goal of 100% non-inductive current fraction has not been reached, due to the low current drive efficiencies at these densities and the low bootstrap current fraction obtained, ~40%, which is mainly produced in the pedestal region. In addition to this problem, it has been shown that very small or vanishing off-axis current is obtained due to the modest amount of LH power, the need to use high $n_{||}$ and the fact that the NBCD is on-axis and rather peaked. These features have a clear implication on the sustainment of these scenarios, the q

profile drops from an initial value close to 2 just before the L-H transition to a final value of 1 at the end of the flat-top phase.

In order to analyze whether more off-axis current can overcome these issues, 10 MW of ECRH/ECCD with a deposition at $\rho = 0.6$ has been considered. Results obtained show that LH power is very useful to drive a weak ITB in the ramp-up phase with $q>2$, however, this is not enough to sustain this scenario in the flat-top phase. On the other hand, when the full ECRH/ECCD power is used, the q profile evolution is highly reduced, with nearly 100% of non-inductive current. The enhancement of the total non-inductive current is obtained by the increase of bootstrap current by 10%, due to the ITB in the ion channel, and by the addition of 0.25MA of ECCD.

This analysis shows the importance of the off-axis current in order to create and sustain advanced steady-state scenarios compatible with ITER features. In particular, and according to the calculations made in this paper, different H&CD schemes of input power and current drive are needed to create a scenario with ITB and to sustain it. In fact, this analysis has shown that with only 2MW of LH it is possible to create a wide ITB scenario if this power is used in the ramp-up phase, however this ITB is lost after 2s. Therefore, more off-axis current is needed, which could be supplied by ECCD. These features have been already pointed out to be important for the ITER steady-state scenario [24-26]. Moreover, the problem of current alignment, which has been identified has critical for the transition to high beta regimes [27], could be easily analyzed in these scenarios, due to the high bootstrap current fraction needed and the necessity of enough off-axis current to generate it. Therefore, the experimental analysis of these problems on JET would be of extreme interest on the way to ITER.

**ACKNOWLEDGEMENTS.**

This work, supported by the European Communities under the contract of Association between EURATOM and CEA, was carried out within the framework of the European Fusion Development Agreement. The views and opinions expressed herein do not necessarily reflect those of the European Commission.

**REFERENCES**

[1]. Gormezano C. et al., Nuclear Fusion **47**, S285 (2007).
[2]. Joffrin E. et al., Plasma Physics and Controlled Fusion **49**, B629 (2007).
[3]. Murakami M. et al, Phys. Rev. Lett. **90**, 25 (2003).
[4]. Suzuki T., Nuclear Fusion **48**, 045002 (2008).
[5]. Artaud J.F. et al., Nuclear Fusion **50**, 043001 (2010).
[6]. Erba M. et al., Plasma Physics and Controlled Fusion **39,** 261 (1997).
[7]. Huysmans G.T.A., Goedbloed J.P. and Kerner W. 1991 *CP90 Conf. on Comp. Physics* (Singapore: Word Scientific) p 371.
[8]. Houlberg W.A. et al., Physics of Plasmas **4,** 3230 (1997).

[9]. Schneider M. et al., submitted to Nuclear Fusion.
[10]. Schneider M. et al., Plasma Physics and Controlled Fusion **47**, 2087 (2005).
[11]. Krivenski V. et al., Nuclear Fusion **25**, 127 (1985).
[12]. Lin-Liu Y.R., Chan V.S. and Prater R., Physics of Plasmas **10,** 4064 (2003).
[13]. Peysson Y. and Decker J., *in Proc. of the 34th EPS conference on Contr. Fusion and Plasma Phys.* (2007), **31F**, P-4.164.
[14]. Eriksson L.-G., Hellsten T. and Willén, U., Nuclear Fusion **33,** 1037 (1993).
[15]. Post D.E. et al., Atom. Data Nuclear Data Tables **20**, 397 (1977).
[16]. Hahm T.S. and Burrell K.H., Physics of Plasmas **2**, 1648 (1995).
[17]. Tala T.J.J. et al, Nuclear Fusion **46**, 548 (2006).
[18]. S.M. Kaye, M. Greenwald and U. Stroth et al., Nuclear Fusion **37,** 1303 (1997).
[19]. Artaud J F et al 2005 Proc. 32nd EPS Conf. on Plasma Physics (Tarragona, Spain) vol 29C (ECA) P-1.035
[20]. Giruzzi G. et al., 23rd IAEA Fusion Energy Conference, 11-16 October 2010, Korea, FTP/P6-11.
[21]. Baranov Yu. Et al., Plasma Physics and Controlled Fusion **47**, 975 (2005).
[22]. Litaudon X. et al., Nuclear Fusion **47**, 1285 (2007).
[23]. Bizarro J.P.S. et al., Nuclear Fusion **47,** L41 (2007).
[24]. Garcia J. et al., Physical Review Letters **100**, 255004 (2008).
[25]. Garcia J. et al., Plasma Physics and Controlled Fusion **50**, 12 (2008).
[26]. Garcia J. et al., Nuclear Fusion **50**, 025025 (2010) .
[27]. Garcia J. et al., Physical Review Letters **104**, 205003 (2010).

| Discharge | $q_{95}$ | $\varkappa/\delta$ | Bt (T) | $\beta_N$ | $n/n_{Gw}$ | Ip (MA) |
|---|---|---|---|---|---|---|
| #77895 | 4.9 | 1.75/0.44 | 2.7 | 2.3 | 0.55 | 1.75 |
| #78052 | 4.7 | 1.75/0.44 | 2.7 | 2.1 | 0.57 | 1.75 |

*Table 1 Main characteristics of Pulse No's: 77895 and 78052*

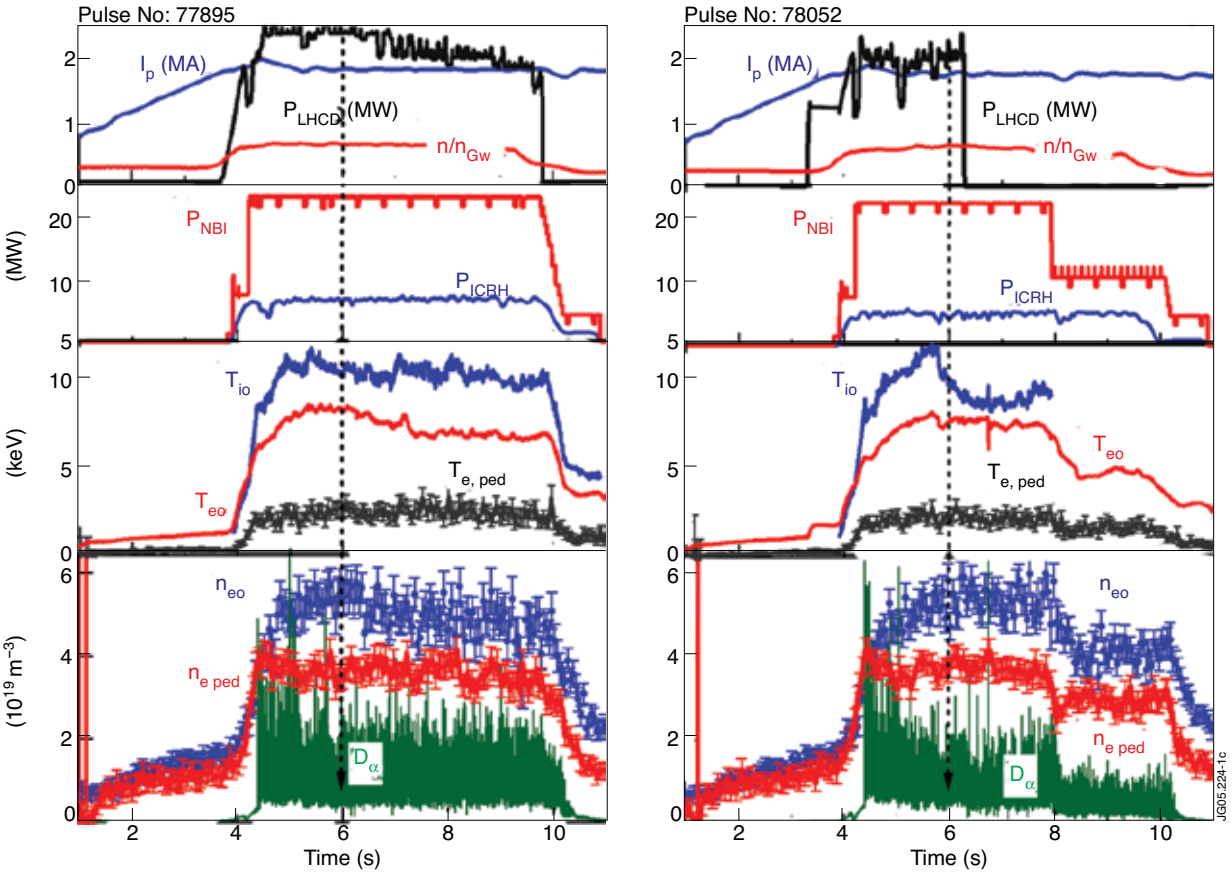


*Figure 1: Time evolution of the main parameters for Pulse No: 77895 (a) Time evolution of the main parameters for Pulse No: 78052 (b). Dashed line corresponds to the time for which the profile analysis is done.*

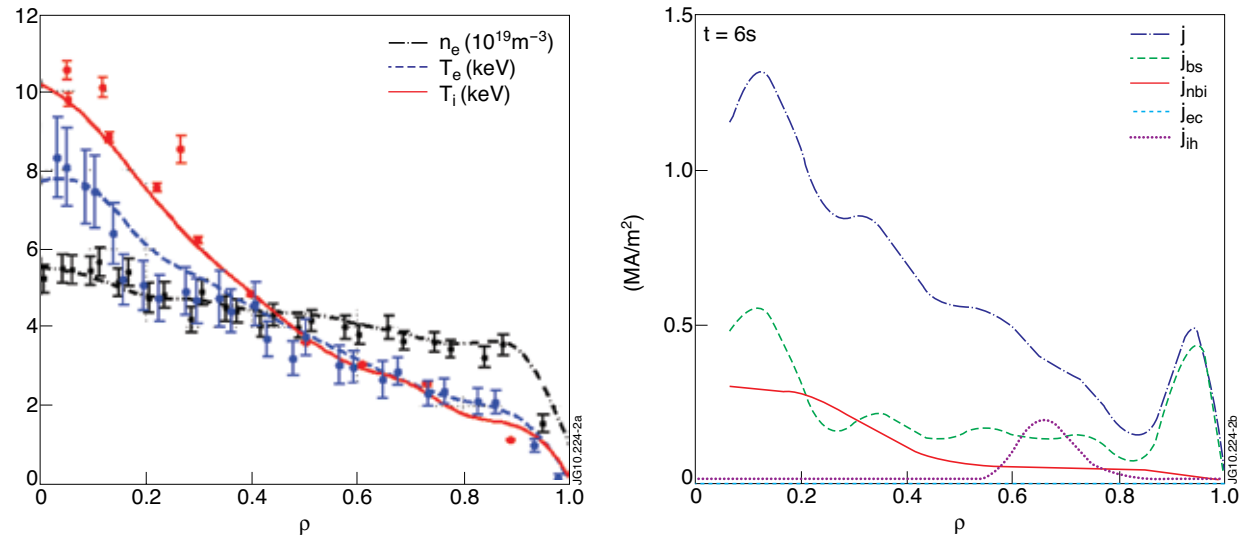


*Figure 2: Electron temperature (Te), ion temperature (Ti) and electron density (ne) profiles at t = 6s (left). Total current (j), bootstrap current ($j_{bs}$), NBCD ($j_{nbi}$) and lower hybrid ($j_{lh}$) current drive density profiles at t = 6s (right).*

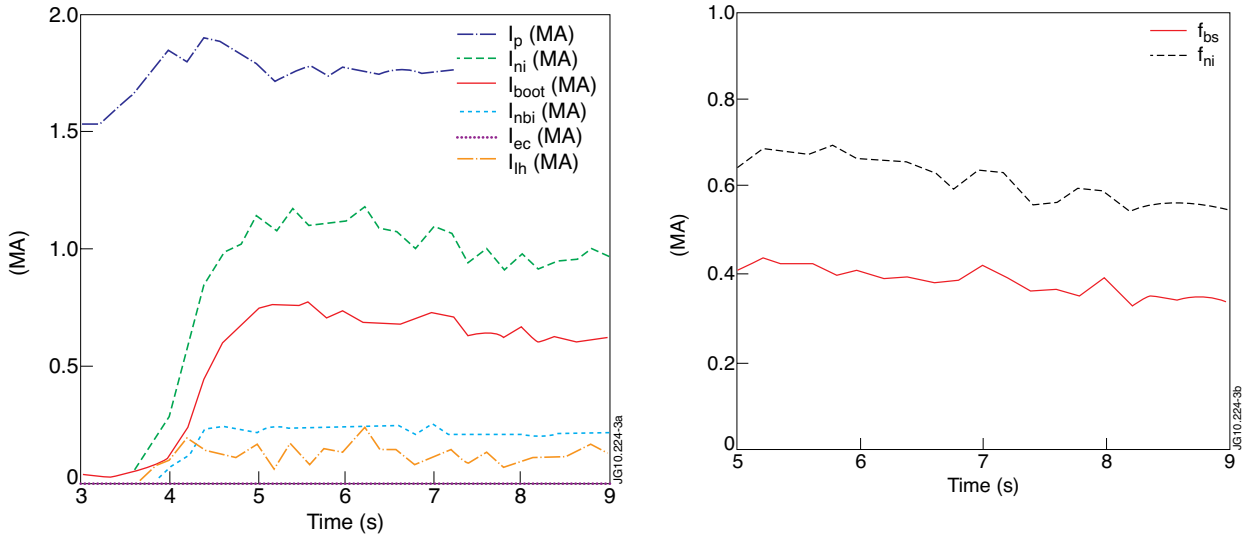


*Figure 3: Evolution of total ($I_p$), non-inductive ($I_{ni}$), bootstrap ($I_{bs}$), NBCD ($I_{nbi}$) and LH ($I_{lh}$) currents (a). Evolution of the bootstrap ($f_{bs}$) and non-inductive ($f_{ni}$) currents fraction (b).*

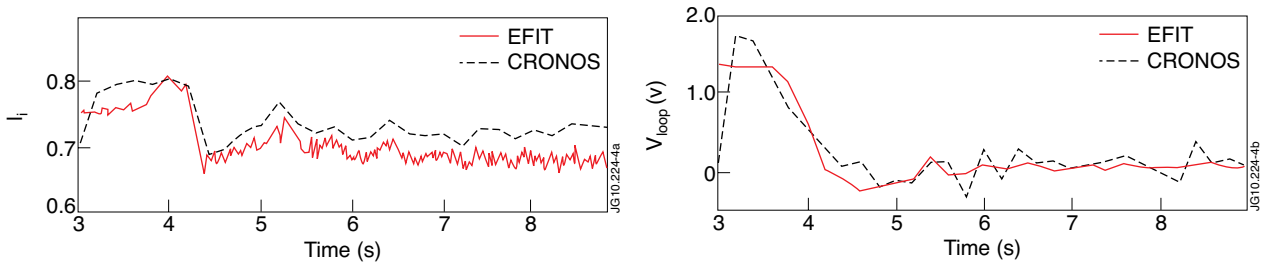


*Figure 4: Comparison between $l_i$ calculated with EFIT and CRONOS (a) Comparison between $V_{loop}$ calculated with EFIT and CRONOS (b).*

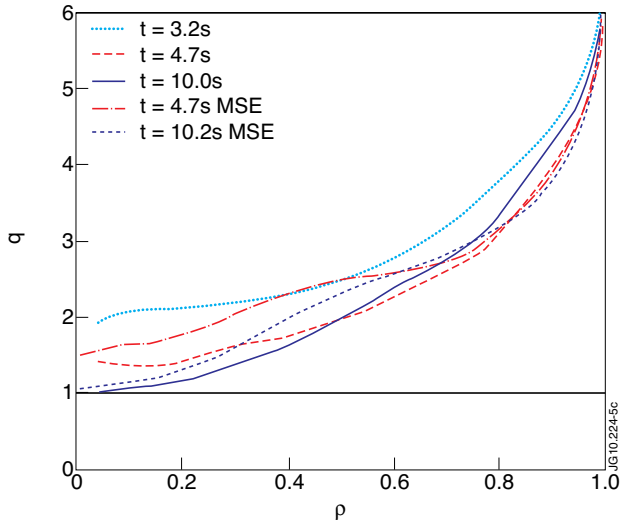


*Figure 5: Comparison between the q profile evolution obtained with CRONOS and the one calculated by EFIT constrained by MSE and total pressure data.*

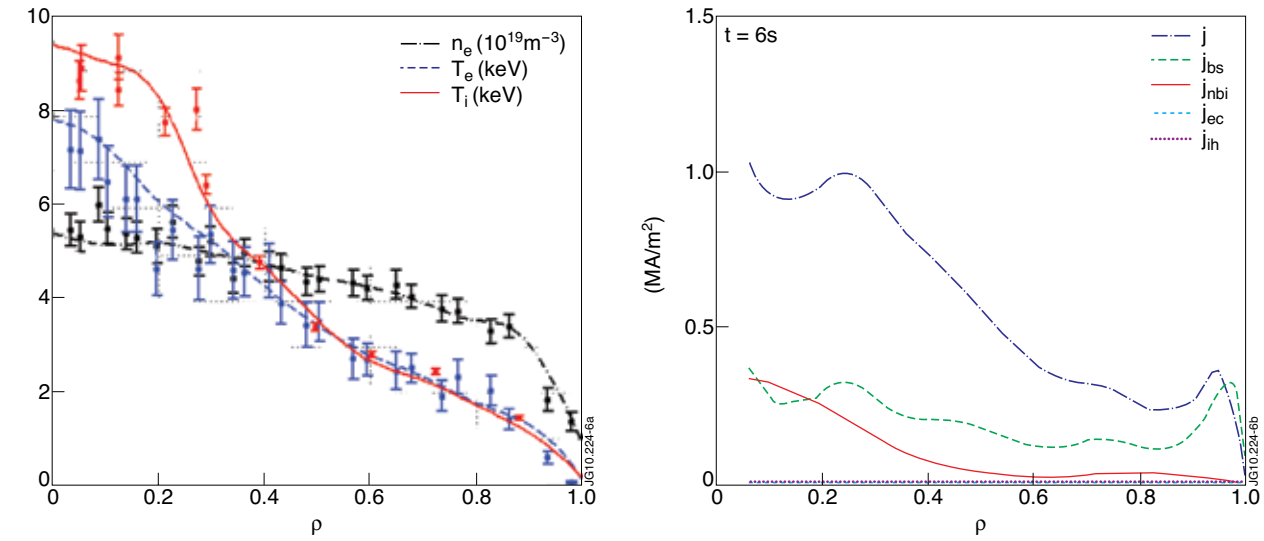


*Figure 6: Electron temperature ($T_e$), ion temperature ($T_i$) and electron density ($n_e$) profiles at t = 6s (left). Total current (j), bootstrap current ($j_{bs}$) and NBCD ($j_{nbi}$) current drive density profiles at t = 6s (right).*

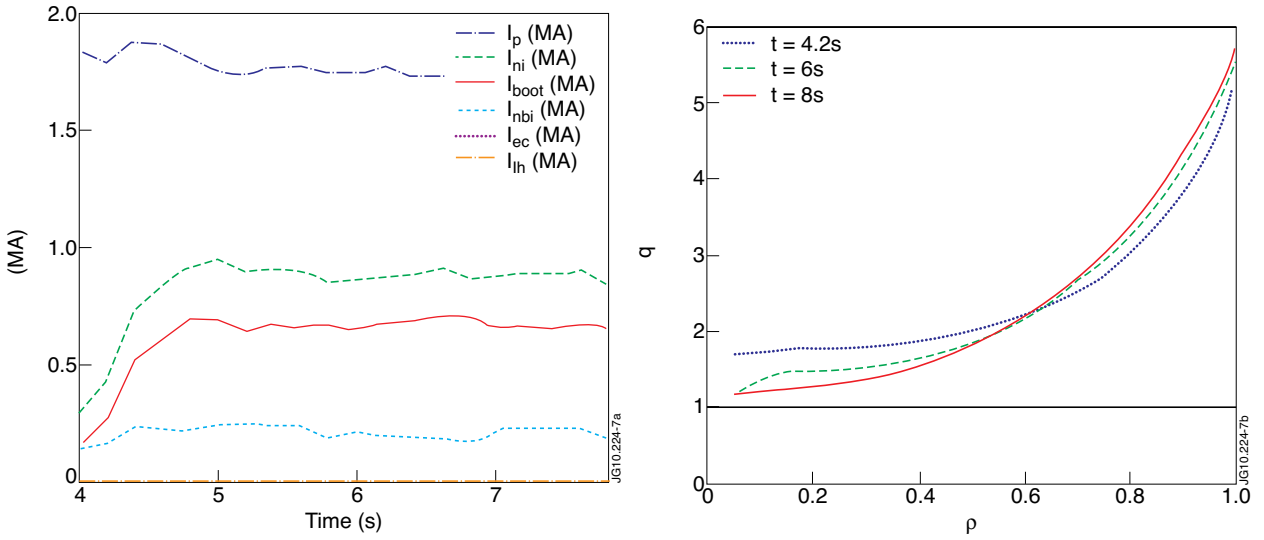


*Figure 7: Evolution of total ($I_p$), non-inductive ($I_{ni}$), bootstrap ($I_{bs}$) and NBCD ($I_{nbi}$) currents (a). Evolution of the q profile (b).*

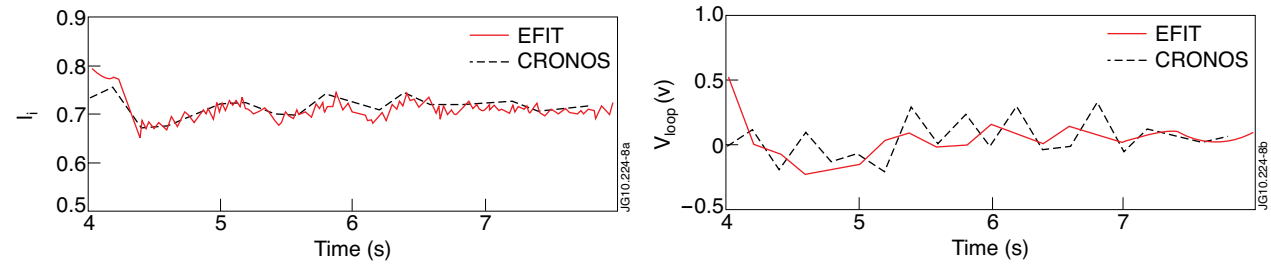


*Figure 8: Comparison between $l_i$ calculated with EFIT and CRONOS (a) Comparison between $V_{loop}$ calculated with EFIT and CRONOS (b).*

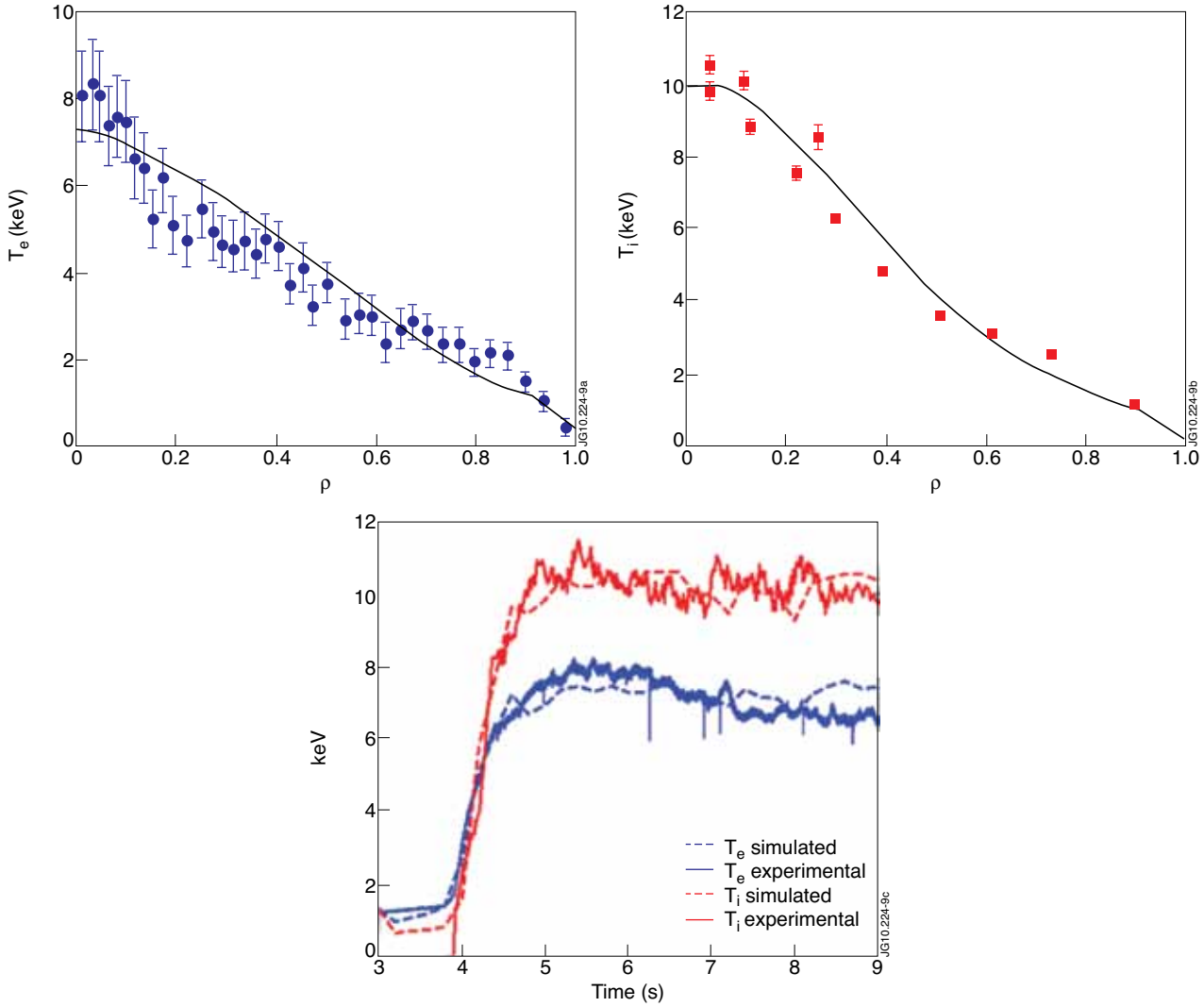


*Figure 9: Comparison between the simulated electron temperature profile and the experimental one at t = 6s (a) Comparison between the simulated ion temperature profile and the experimental one at t = 6s (b) Comparison between the time evolution of the simulated electron and ion central temperatures and the experimental ones (c).*

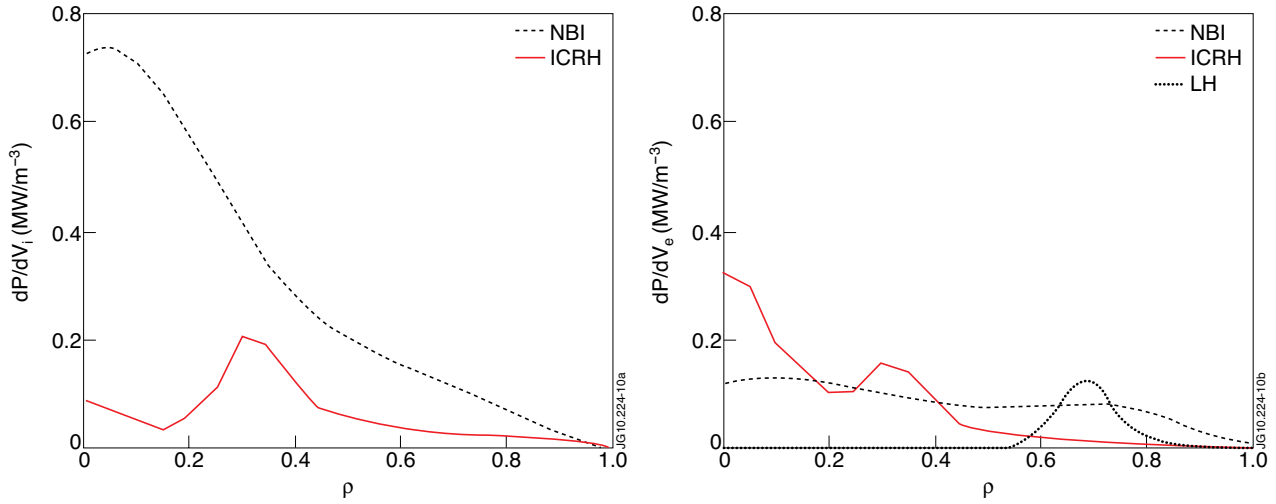


*Figure 10: Input power density profiles for the ions (a) Input power density profiles for the electrons (b).*

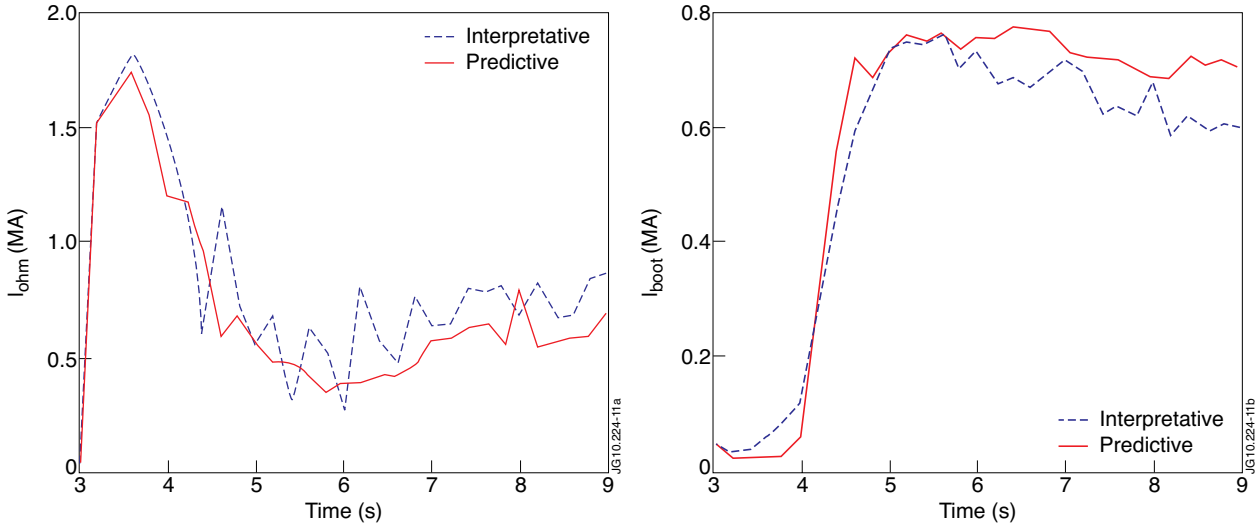


*Figure 11: Comparison between the predictive and interpretative total ohmic current (a) Comparison between the predictive and interpretative total bootstrap current (b).*

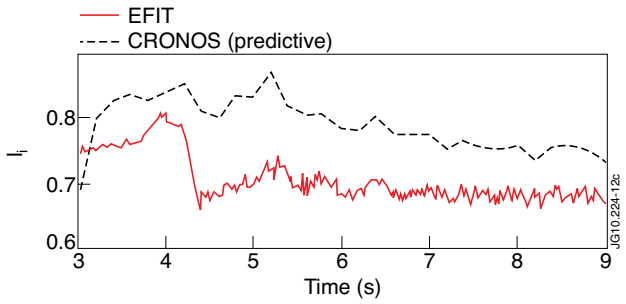


*Figure 12: Comparison between li calculated with EFIT and the one obtained with the full simulation made with CRONOS.*

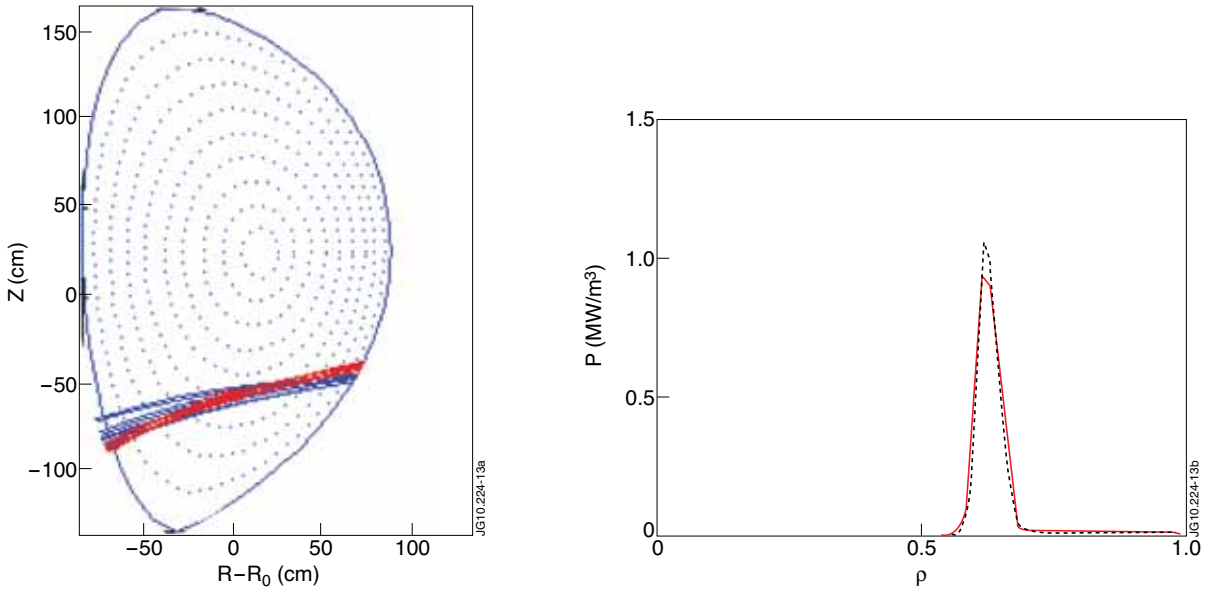


*Figure 13: Poloidal projection of ray trajectories for both launchers (a) Power density profile deposition (b).*

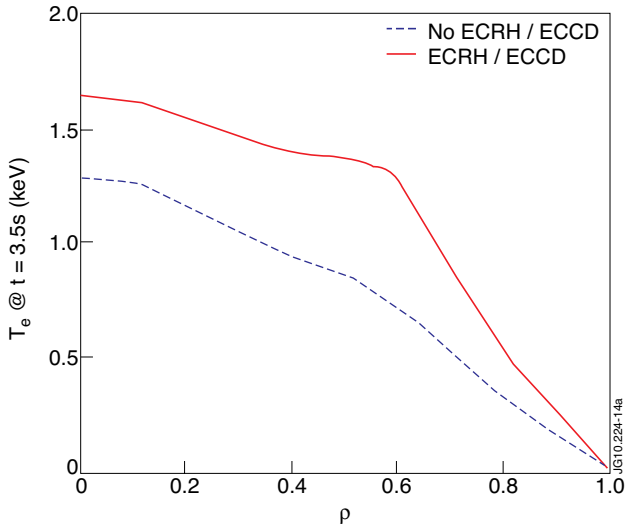


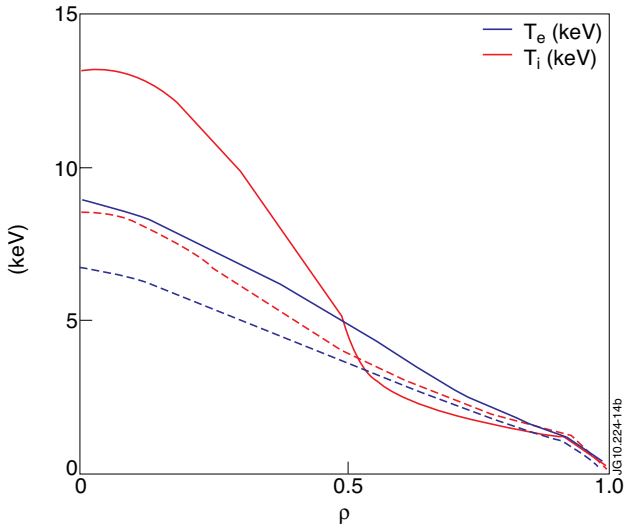


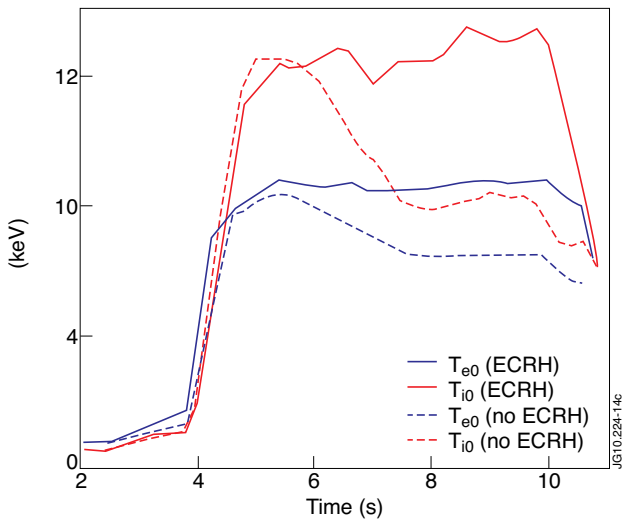


*Figure 14: Comparison between the electron temperature obtained with ECRH/ECCD and no ECRH/ECCD heating at t = 3.5s (a) Comparison between temperature profiles obtained in scenario 1 and scenario 2 at t=6s (b) Comparison between the evolution of the central temperatures in scenario 1 and scenario 2 (c).*

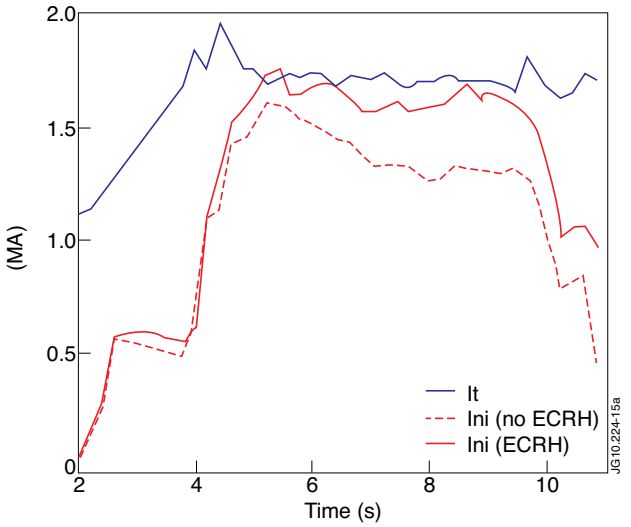


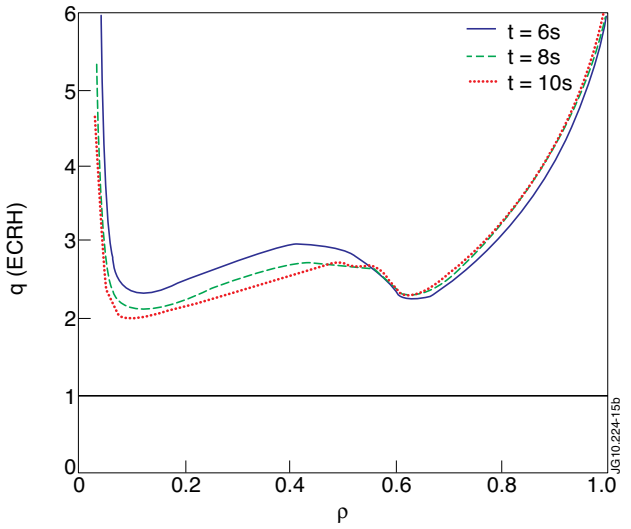


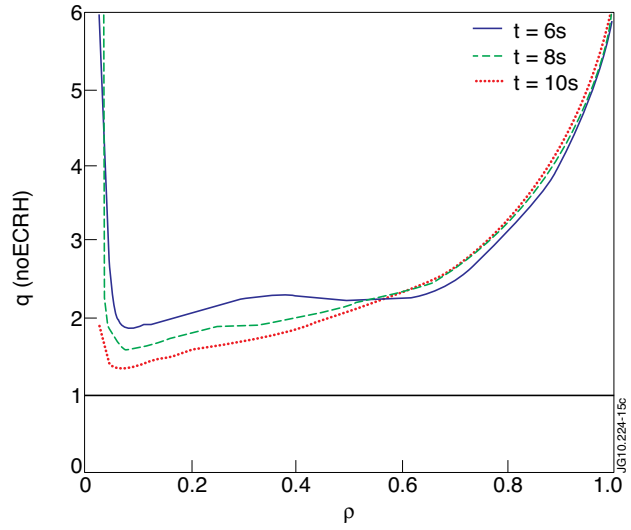


*Figure 15: Evolution of the total current (It) and the non-inductive current for scenario 1 and scenario 2 (a) Evolution of the q profile for scenario 2 (b) Evolution of the q profile for scenario 1 (c).*

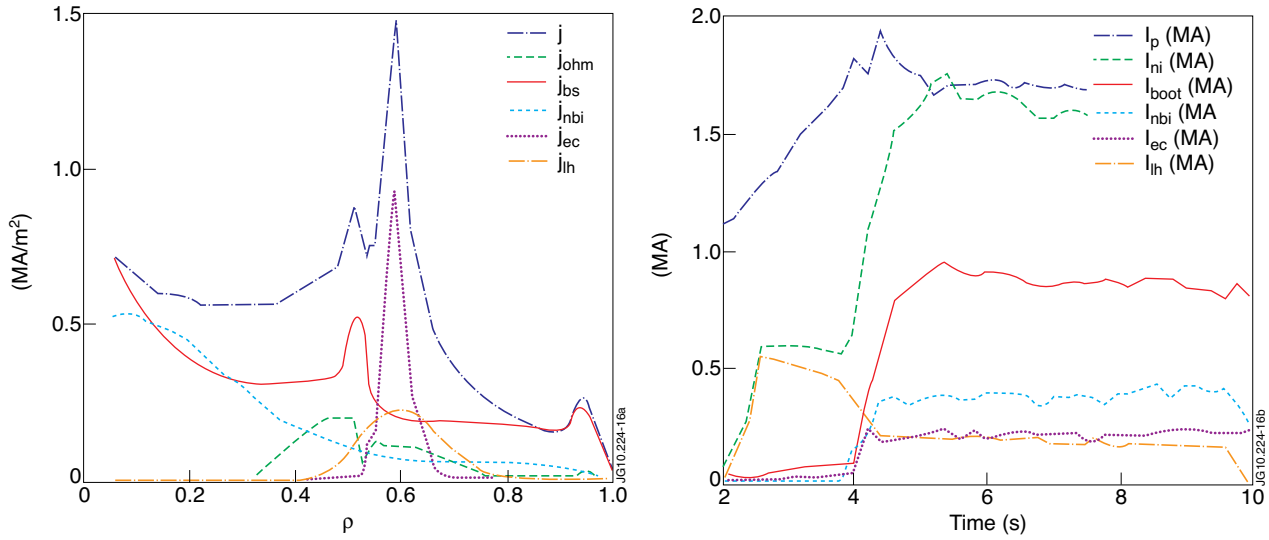


*Figure 16: Total current (j),ohmic current (johm), bootstrap current (jbs), NBCD (jnbi), ECCD (jec) and lower hybrid (jlh) current drive density profiles at t=6s for scenario 2(a) Evolution of total (Ip), non-inductive (Ini), bootstrap (Ibs), NBCD (Inbi), ECCD (Iec) and LH (Ilh) currents (b).*

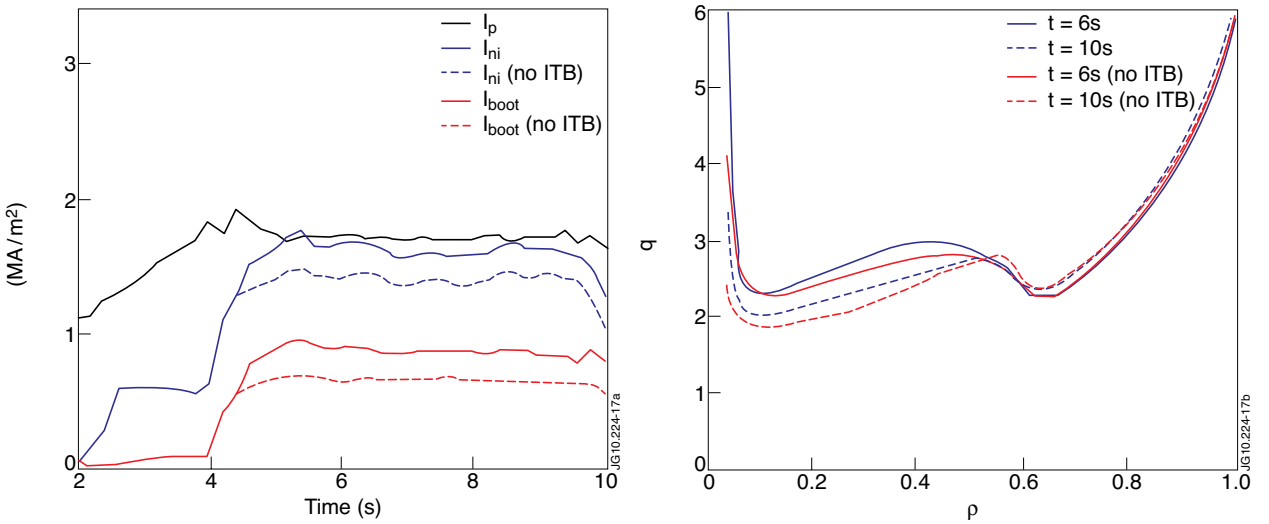


*Figure 17: Comparison between the total current ($I_p$), the non-inductive current ($I_{ni}$), and the bootstrap current ($I_{boot}$), in the case of scenario 2 with ITB and no ITB (left) Comparison between the evolution of the q profile in the case of scenario 2 with ITB and no ITB (right).*

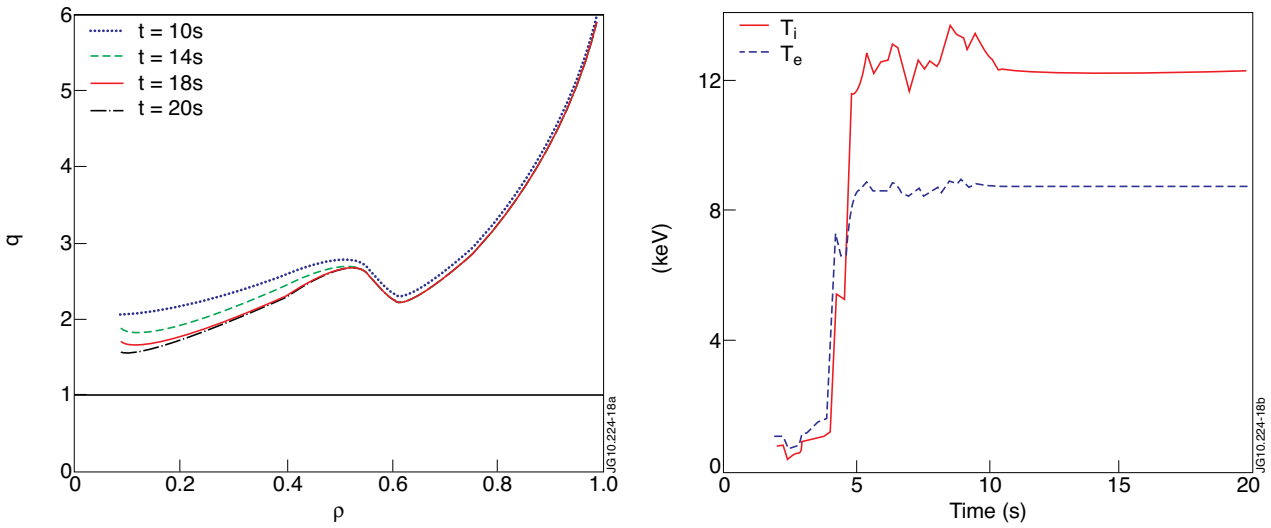


*Figure 18: Evolution of the q profile for scenario 2 extended up to 20s(a). Evolution of central temperatures for scenario 2 extended up to 20s (b).*